Available online at www.sciencedirect.com

ScienceDirect

Advances in Space Research 53 (2014) 1313–1328

ADVANCES IN SPACE RESEARCH (a COSPAR publication)

www.elsevier.com/locate/asr

Investigation of ionospheric response to two moderate geomagnetic storms using GPS–TEC measurements in the South American and African sectors during the ascending phase of solar cycle 24

A.J. de Abreu [a,*], P.R. Fagundes [a], M. Gende [b], O.S. Bolaji [c], R. de Jesus [a], C. Brunini [b]

[a] *Departamento de Física e Astronomia, Universidade do Vale do Paraíba (UNIVAP), São José dos Campos, São Paulo, Brazil*
[b] *Facultad de Ciencias Astronómicas y Geofísicas, Universidad Nacional de La Plata (UNLP), La Plata, Argentina*
[c] *Department of Physics, University of Lagos, Akoka, Lagos, Nigeria*

Received 24 December 2013; received in revised form 5 February 2014; accepted 11 February 2014
Available online 22 February 2014

Abstract

The responses of the ionospheric F region using GPS–TEC measurements during two moderate geomagnetic storms at equatorial, low-, and mid-latitude regions over the South American and African sectors in May 2010, during the ascending phase of solar cycle 24, are investigated. The first moderate geomagnetic storm studied reached a minimum Dst value of −64 nT at 1500 UT on 02 May 2010 and the second moderate geomagnetic storm reached a minimum Dst value of −85 nT at 1400 UT on 29 May 2010. In this paper, we present vertical total electron content (VTEC) and phase fluctuations (in TECU/min) from Global Positioning System (GPS) observations from the equatorial to mid-latitude regions in the South American and African sectors. Our results obtained during these two moderate geomagnetic storms from both sectors show significant positive ionospheric storms during daytime hours at the equatorial, low-, and mid-latitude regions during the main and recovery phases of the storms. The thermospheric wind circulation change towards the equator is a strong indicator that suggests an important mechanism is responsible for these positive phases at these regions. A pre-storm event that was observed in the African sector from low- to the mid-latitude regions on 01 May 2010 was absent in the South American sector. This study also showed that there was no generation or suppression of ionospheric irregularities by storm events. Therefore, knowledge about the suppression and generation of ionospheric irregularities during moderate geomagnetic storms is still unclear.

Keywords: Geomagnetic storm; Ionosphere; F region; GPS

1. Introduction

Studies related to space weather in the Sun–Earth system are of great relevancies to our modern technologies. The Sun–Earth interaction drastically affects the magnetosphere–ionosphere–thermosphere system causing varieties of physical phenomena, which include geomagnetic storms and ionospheric disturbances. Geomagnetic storms usually result from increase in speed and/or density of the solar wind due to coronal mass ejections (CMEs), which can be associated or not with solar eruptions (Gonzalez and Tsurutani, 1987; Tsurutani and Gonzalez, 1997). This increase in speed and/or density of the solar wind characterizes the initial phase of a geomagnetic storm or sudden storm commencement (SSC) (Willis, 1964). SSC is not a necessary condition for development of a geomagnetic storm, because a geomagnetic storm could occur and

* Corresponding author. Tel.: +55 12 39312664.
E-mail address: abreu.alessandro@gmail.com (A.J. de Abreu).

http://dx.doi.org/10.1016/j.asr.2014.02.011
0273-1177/

develop with a gradual storm commencement (GSC) (Mendillo, 2006). Geomagnetic storms also have a main phase and a recovery phase (Kumar et al., 2005). During the main phase, the energy input into the upper atmosphere in high latitude is maximized due to the magnetic reconnection process. This is because of the *Bz* interplanetary magnetic field, which turns southward to interconnect with the geomagnetic field (Tsurutani et al., 2004). However, during the recovery phase, the energy input minimizes and the geomagnetic activity decreases (Schunk and Nagy, 2000). During periods of moderate and intense geomagnetic storms, ionospheric disturbances are observed at the equatorial, low-, and mid-latitude regions (Burns et al., 1995a; Richmond and Lu, 2000). A positive ionospheric storm (positive phase) observed on ionospheric parameters, which is due to these disturbances, results from an increment in the electron density. Otherwise, a decrease in the electron density of the ionospheric parameter is referred to as negative ionospheric storm (negative phase) (Danilov and Morozova, 1985; Prolss, 1993; Bauske and Prolss, 1998; Prolss and Werner, 2002). Werner et al. (1999), Basu et al. (2001), Sastri et al. (2002), Tsurutani et al. (2004), Basu et al. (2007), Fejer et al. (2007), Balan et al. (2010), Klimenko et al. (2011), de Jesus et al. (2013), Huang (2013), and Simi et al. (2013) found that drastic change in the equatorial, low-, and mid-latitude of the ionospheric F region can be produced by intense disturbance of electric fields and global winds that originated from magnetosphere–ionosphere interaction. These electric fields are identified by prompt or direct equatorward penetration of magnetospheric electric fields from high latitude region (a few hours) and disturbance of dynamo electric fields (several hours) generated by the global winds circulation due to the Joule heating in the high latitude atmosphere, which are consequences of particle precipitation (Abdu, 1997; Richmond et al., 2003; Maruyama et al., 2005; Zaka et al., 2010; Klimenko and Klimenko, 2012). The effects of the electric fields in the equatorial region may increase or decrease the F region height. The increase or decrease of the F region height modifies the speed of electromagnetic drifts ($\mathbf{E} \times \mathbf{B}$) may affect the ionization at low latitudes (Abdu et al., 1993). The changes in the global winds circulation (blowing from high latitudes to the equatorial regions), generated by Joule heating, can also modify the ionosphere–thermosphere system. This modification could raise the F region to higher altitudes such that the neutral composition is influenced (Fuller-Rowell et al., 1994). In addition, the Joule heating can drive the propagation of atmospheric gravity waves towards the equator in the form of traveling atmospheric disturbances (TADs). These TADs, when they interact with the ionosphere, could produce traveling ionospheric disturbances (TIDs) (Killeen et al., 1984; Fagundes et al., 1995; de Abreu et al., 2010a). Some studies worth mentioning are the work of Whalen (2002), Sahai et al. (2007a, 2009a,b,c), Karpachev et al. (2010), de Jesus et al. (2010, 2012), and de Abreu et al. (2011). They investigated generations and suppressions of equatorial spread-F (ESF) at the equatorial, low-, and mid-latitude regions of the ionospheric F region during geomagnetic disturbances. Sahai et al. (2007a), using ionosonde data in the Brazilian sector, observed bottomside spread-F only during the main phase of the storm, whereas that during the recovery phase, they observed large-scale plasma bubble. de Jesus et al. (2010), using ionosonde data in the South American sector, observed plasma bubbles in the mid-latitude regions after the rapid uplifting of the F-region in the equatorial and low latitude regions.

In this investigation, we present and discuss responses of the ionospheric F region using GPS–TEC measurements at equatorial, low-, and mid-latitude regions in the South American and African sectors to two moderate geomagnetic storms in May 2010 during the ascending phase of solar cycle 24. The ionospheric responses during geomagnetic storms at different latitudes and longitudes have been

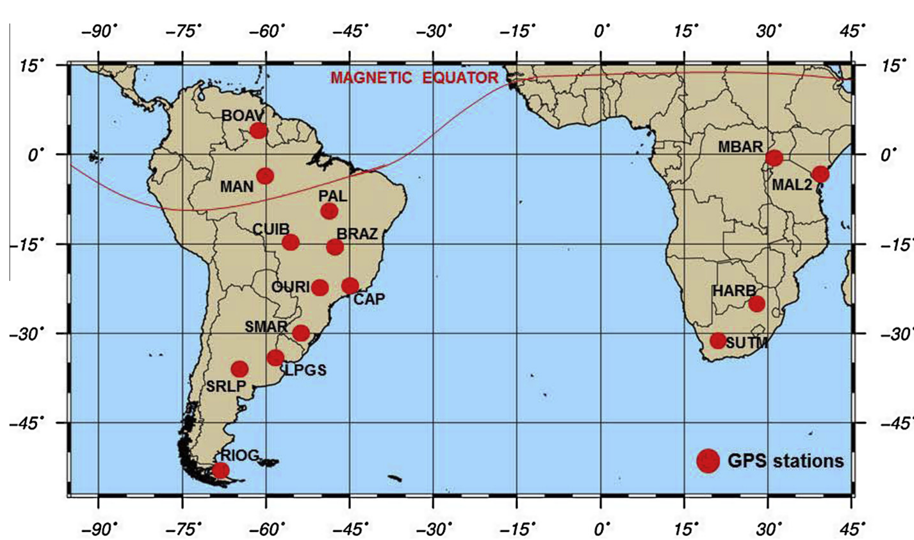

Fig. 1. A map showing the locations of the GPS stations used in the present study. The geographic and magnetic equators are also shown.

Table 1
Details of the Global Positioning System (GPS) sites used in the present study.

Location	Symbol used (Network)	Geog. Lat.	Geog. Long.	Dip Lat.	Local time (LT)
Boa Vista	BOAV (RBMC)	02.8°N	60.7°W	10.5°N	LT = UT − 4 h
Manaus	MAN (RBMC)	02.9°S	60.0°W	05.1°N	LT = UT − 4 h
Palmas	PAL (RBMC)	10.2°S	48.2°W	07.0°S	LT = UT − 3 h
Cuiabá	CUIB (RBMC)	15.6°S	56.1°W	07.7°S	LT = UT − 4 h
Brasília	BRAZ (RBMC)	15.9°S	47.9°W	12.0°S	LT = UT − 3 h
Cachoeira Paulista	CAP (RBMC)	22.7°S	45.0°W	19.0°S	LT = UT − 3 h
Ourinhos	OURI (RBMC)	22.9°S	49.9°W	16.6°S	LT = UT − 3 h
Santa Maria	SMAR (RBMC)	29.7°S	53.7°W	19.9°S	LT = UT − 3 h
La Plata	LPGS (SIRGAS)	34.9°S	57.9°W	22.0°S	LT = UT − 4 h
Santa Rosa, La Pampa	SRLP (SIRGAS)	36.6°S	64.3°W	21.7°S	LT = UT − 4 h
Rio Grande	RIOG (SIRGAS)	53.8°S	67.8°W	30.6°S	LT = UT − 4 h
Uganda	MBAR (IGS)	00.6°S	30.7°E	12.3°S	LT = UT + 3 h
Kenya	MAL2 (IGS)	03.0°S	40.1°E	13.6°S	LT = UT + 3 h
Pretória	HARB (IGS)	25.9°S	27.7°E	42.1°S	LT = UT + 2 h
Sutherland	SUTM (IGS)	32.4°S	20.8°E	45.8°S	LT = UT + 2 h

studied by Namgaladze et al. (2000), Goncharenko et al. (2005), de Abreu et al. (2010b), Klimenko et al. (2011), Sahai et al. (2011), Amabayo et al. (2012), Ngwira et al. (2012), and Uma et al. (2012). Namgaladze et al. (2000) used numerical simulations of the upper atmosphere model to carry out their investigations of low solar activity year 1974 during a moderate geomagnetic storm. They suggested that a positive phase of the ionospheric storm is mainly caused by large-scale neutral wind circulation and the passage of the TIDs. de Abreu et al. (2010b) also observed similar positive ionospheric storm phase when they investigated April 2000 super-storm using GPS measurements. They ascribed the mechanism responsible for a positive ionospheric storm to the role played by meridional wind at the equatorial and low latitude regions of the Brazilian sector. Amabayo et al. (2012) observed the storm-induced TEC perturbations from 11 to 12 April 2001, and they attributed these irregularities over South Africa to influence of TIDs. Uma et al. (2012) used ionosondes, global ionospheric maps and ground-based GPS receivers of TEC, satellite, and empirical model to study the ionospheric response over Japanese and Indian longitude sectors during two geomagnetic storms that occurred on 31 March, 2001 and 20 November, 2003. They observed that the equatorial ionization anomaly is expanded and intensified during the main phase of these two storms, which is believed to be caused by the prompt penetration of electric field. They also observed that the storm associated thermospheric wind is propagating equatorward during the recovery phase that is responsible for a height rise in

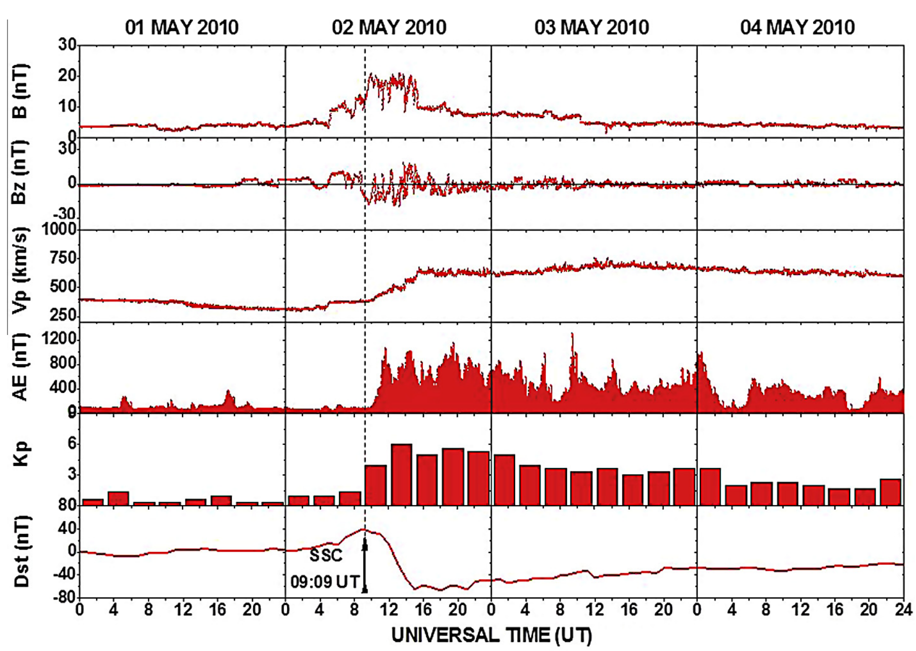

Fig. 2. Variations of the total interplanetary magnetic field (IMF) *B*, *z* component of IMF *Bz* in GSM coordinates, and solar wind proton bulk velocity *Vp*, obtained from the ACE satellite during the period 01–04 May 2010. The AE, *Kp*, and Dst geomagnetic indices during the period 01–04 May 2010 are also presented. The black vertical arrow and dashed line indicate the sudden storm commencement (SSC).

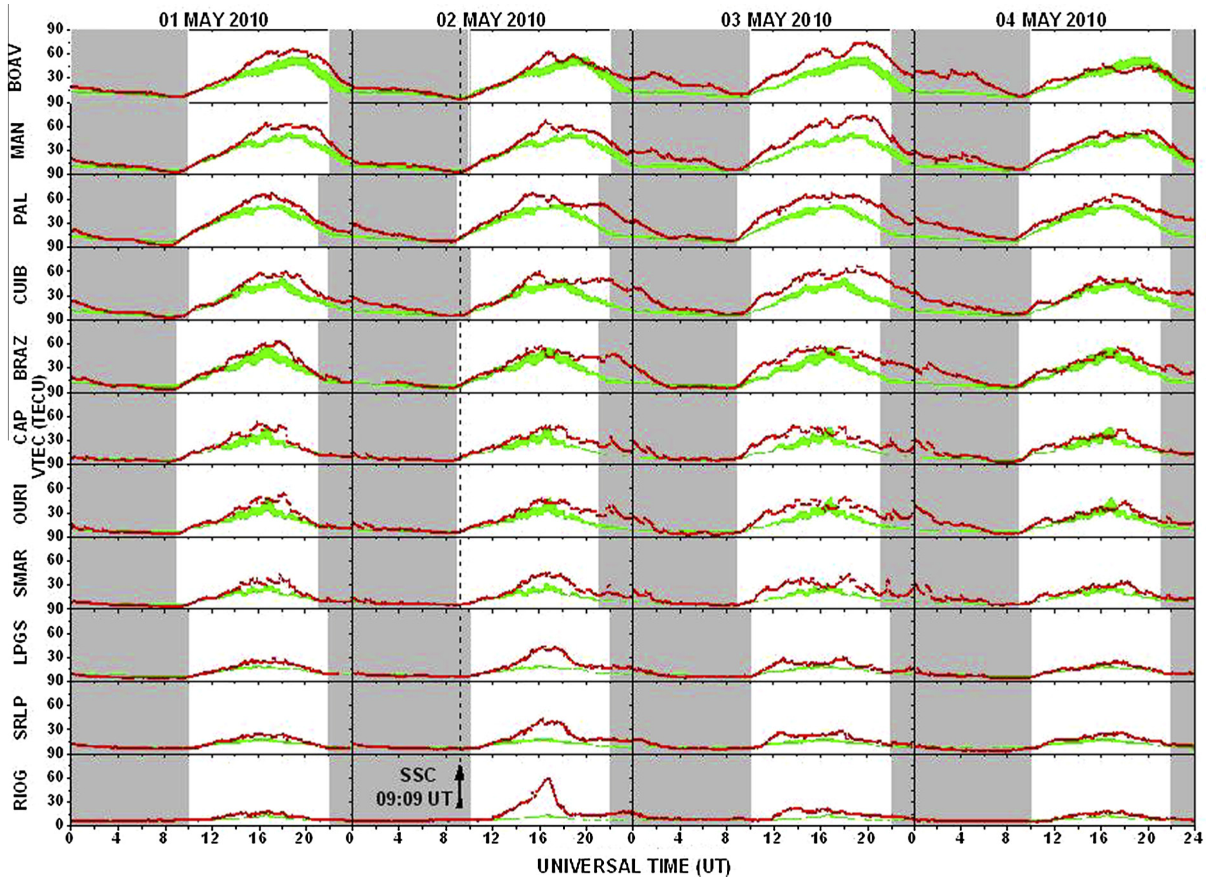

Fig. 3. Variations of the vertical total electron content (VTEC) from GPS observations obtained from different satellites at 11 receiving stations in the South American sector during the period 01–04 May 2010 (red lines). The green bands are ±1 standard deviation of the average quiet day (four quiet days) values. The black vertical arrow and dashed line indicates the sudden storm commencement (SSC). (For interpretation of the references to color in this figure legend, the reader is referred to the web version of this article.)

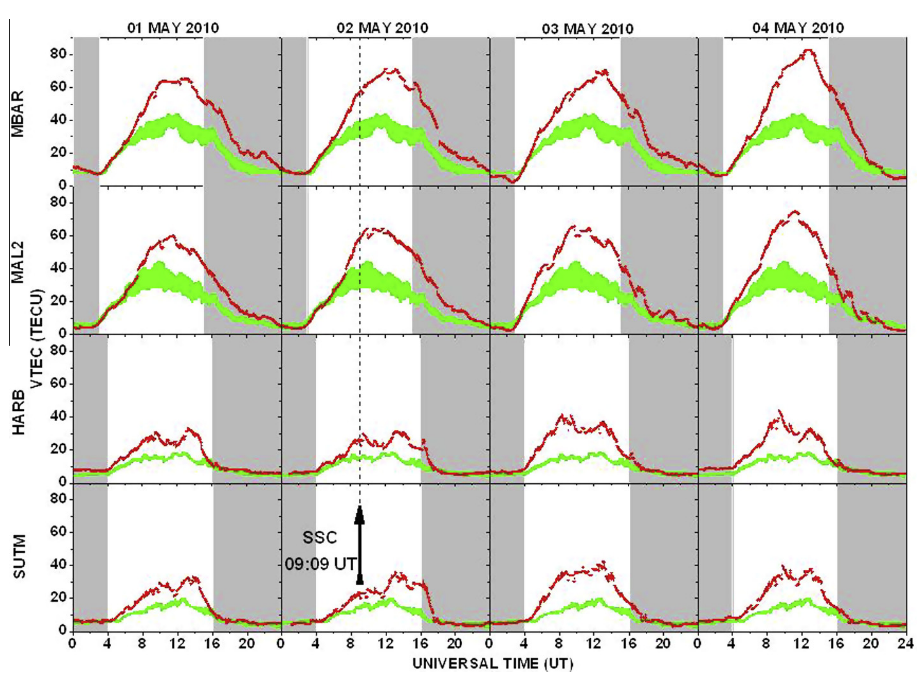

Fig. 4. Variations of the vertical total electron content (VTEC) from GPS observations obtained from different satellites at 04 receiving stations in the African sector during the period 01–04 May 2010 (red lines). The green bands are ±1 standard deviation of the average quiet day (four quiet days) values. The black vertical arrow and dashed line indicates the sudden storm commencement (SSC). (For interpretation of the references to color in this figure legend, the reader is referred to the web version of this article.)

the virtual height of the F-region starting from mid to low and equatorial latitudes. For this work, we deduced VTEC from the GPS observations at the equatorial, low-, and mid-latitude regions of the South American and African sectors to investigate ionospheric responses. To the best of our knowledge, this is the first time that simultaneous ionospheric data are used from both sectors to investigate their responses with respect to moderate geomagnetic storms. This will provide us the rare opportunity to compare broad latitudinal and longitudinal range responses in the South American and African sectors during these two moderate geomagnetic storms.

2. Observations and methodology

The Global Positioning System (GPS) data for the 15 stations investigated were retrieved in standard Receiver Independent Exchange (RINEX) format. Fig. 1 and Table 1 provide details of the GPS sites used in the present study. The GPS observations (in RINEX format) were used to obtain the vertical total electron content (VTEC) in unit of TEC (1 TECU = 10^{16} electrons/m^2) (Wanninger, 1993; Sahai et al., 2007b) and the phase fluctuations (rate of change of TEC) in TECU/min (Aarons et al., 1996). The TEC is calculated using the GPS observables of dual-frequency carrier-phase, which were extensively discussed in detail by Brunini et al. (2008). This idea to calculate TEC was obtained based on the fact that the range-delay experience within the ionosphere when radio signal is travelling were observed from the GPS measurements and is proportional to the slant TEC (sTEC) along the satellite–receiver line-of-sight and inversely proportional to the square of the signal frequency. Therefore, subtraction of simultaneous observations at different frequencies leads to observables such that all frequencies, which independently disappear, but the ionospheric and other frequency-dependent effects remain present (Brunini et al., 2008):

$$L_{I,arc} = \text{sTEC} + B_R + B^S + C_{arc} + \varepsilon_L, \quad (1)$$

where $L_{I,arc}$ is the carrier-phase ionospheric observable; the sub-indices *arc* refers to every continuous arc of carrier-phase observations, which are defined as a group of consec-

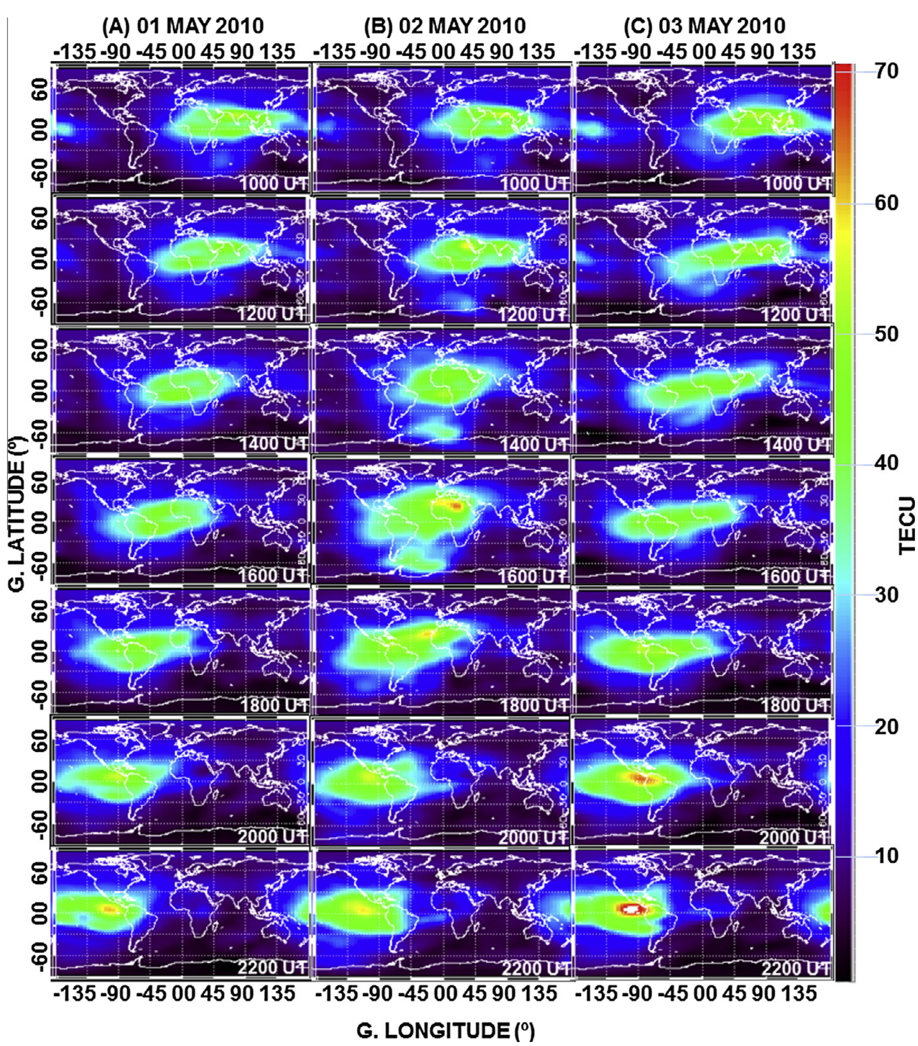

Fig. 5. Twenty-one GPS–TEC maps during the geomagnetic storm on (A) 01 May (geomagnetically quiet) and (B and C) 02–03 May (geomagnetically disturbed).

utive observations that carrier-phase ambiguities do not change; B_R and B^S are the satellite and receiver inter-frequency biases (IFB) for carrier-phase observations; C_{arc} is the bias produced by carrier-phase ambiguities in the ionospheric observable; and ε_L is the effect of noise and multi-path. All terms in Eq. (1) are expressed in Total Electron Content Unit (TECU). Hence, the vertical TEC (VTEC) is given by Brunini et al. (2008) as follows;

$$\mathrm{VTEC} = \cos(z')\mathrm{TEC}, \tag{2}$$

where the value of z', which is the zenith angle of the signal path on the ionospheric pierce point (IPP) located on an average altitude plan H_m, is obtained by:

$$sen\, z' = \frac{R_m}{R_m + H_m} sen\, z, \tag{3}$$

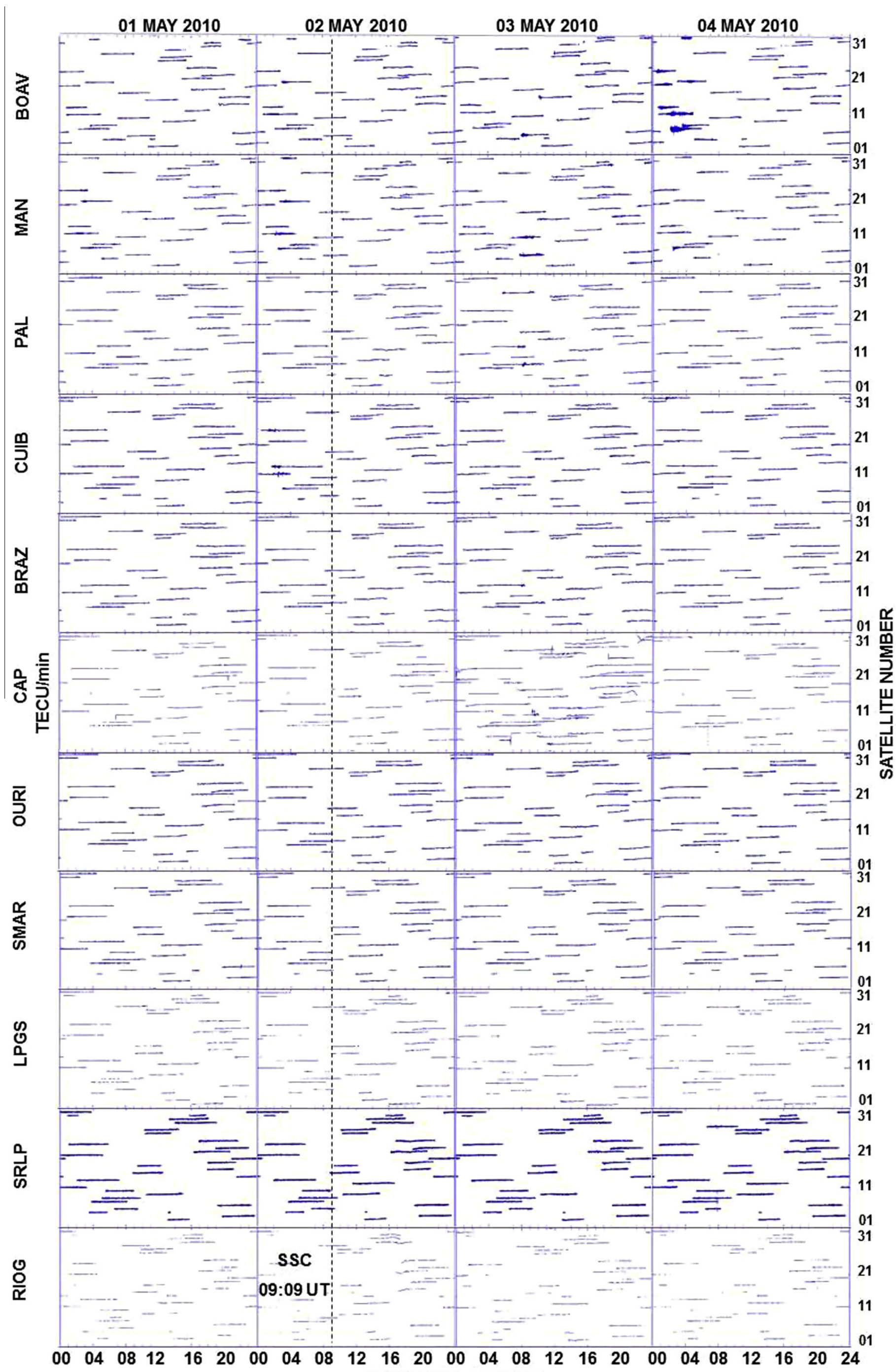

Fig. 6. The phase fluctuations (rate of change of TEC) from GPS observations obtained from different satellites at 11 receiving stations in the South American sector during the period 01–04 May 2010. The black vertical dashed line indicates the sudden storm commencement (SSC).

where R_m is the mean radius of the Earth (6570 km), H_m is the average height of the ionosphere (300 km), and z is the zenith angle of the satellite ($z = 90 - el$, where el is the elevation angle of the satellite). As earlier mentioned, the phase fluctuations are defined by the rates of change of TEC (ROT) in TECU/min, which indicate the presence of the ionospheric irregularities in order of kilometers (Aarons et al., 1996, 1997), which are obtained as follows:

$$\mathrm{ROT} = \frac{\Delta \mathrm{TEC}}{\Delta t}, \tag{4}$$

where ΔTEC is the difference between consecutive $\mathrm{TECs}_{\mathrm{initial}}$ (initial) and $\mathrm{TECs}_{\mathrm{final}}$ (final), which are separated by their simultaneous period differences (Δt), in seconds.

The GPS stations covering from the equatorial to mid-latitude regions in the South American and African sectors

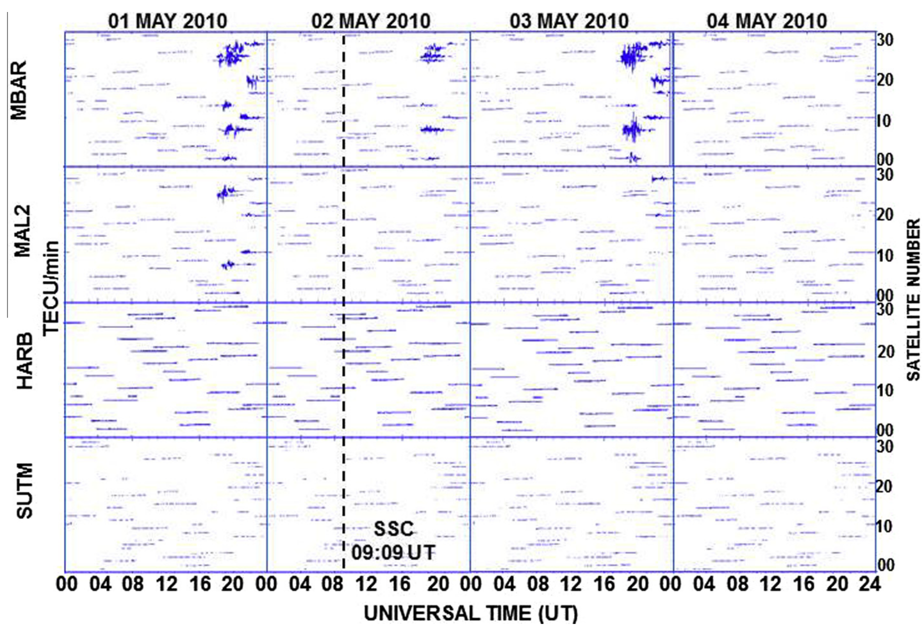

Fig. 7. The phase fluctuations (rate of change of TEC) from GPS observations obtained from different satellites at 04 receiving stations in the African sector during the period 01–04 May 2010. The black vertical dashed line indicates the sudden storm commencement (SSC).

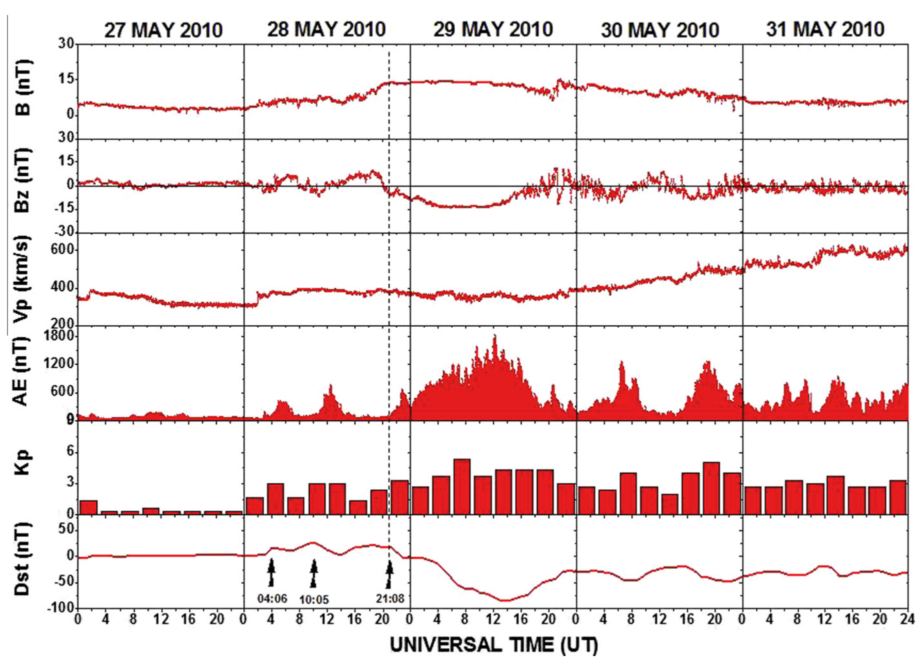

Fig. 8. Variations of the total interplanetary magnetic field (IMF) B, z component of IMF Bz in GSM coordinates, and solar wind proton bulk velocity Vp, obtained from the ACE satellite during the period 27–31 May 2010. The AE, Kp, and Dst geomagnetic indices during the period 27–31 May 2010 are also presented. The black vertical arrow and dashed line indicate the gradual storm commencement (GSC).

are described below. The Boa Vista (BOAV), Manaus (MAN), Palmas (PAL), Cuiabá (CUIB), Brasília (BRAZ), Cachoeira Paulista (CAP), Ourinhos (OURI), and Santa Maria (SMAR) are Brazilian stations, which belong to the "Rede Brasileira de Monitoramento Contínuo (RBMC)" and are operated by the "Instituto Brasileiro de Geografia e Estatística (IBGE)". The La Plata (LPGS), Santa Rosa (SRLP), and Rio Grande (RIOG) are Argentine stations and are operated by the "Serviço de Referência Geocêntrico para as Américas (SIRGAS)". The Uganda (MBAR), Kenya (MAL2), Pretória (HARB), and Sutherland (SUTM) are African stations that are operated by the International Global Navigation Satellite System (GNSS) Service (IGS) and were originally meant for Geodynamics studies (Dow et al., 2005). The stations located in Brazil and Argentina cover the South American sector from equatorial to the mid-latitudes regions. The stations located in Africa cover the low- and mid-latitudes regions. It should be mentioned that the two longitudinal sectors under investigation differ by about 5 h (h) and 7 h in local time (LT) (for more details, see Table 1). The GPS-based TEC maps produced at the Jet Propulsion Laboratory were obtained from http://cdaweb.gsfc.nasa.gov/sp_phys/. The intensity of geomagnetic indices of the auroral electrojet every 1-min values (AE) and intensity of the ring currents hourly values (Dst) used in the present inves-

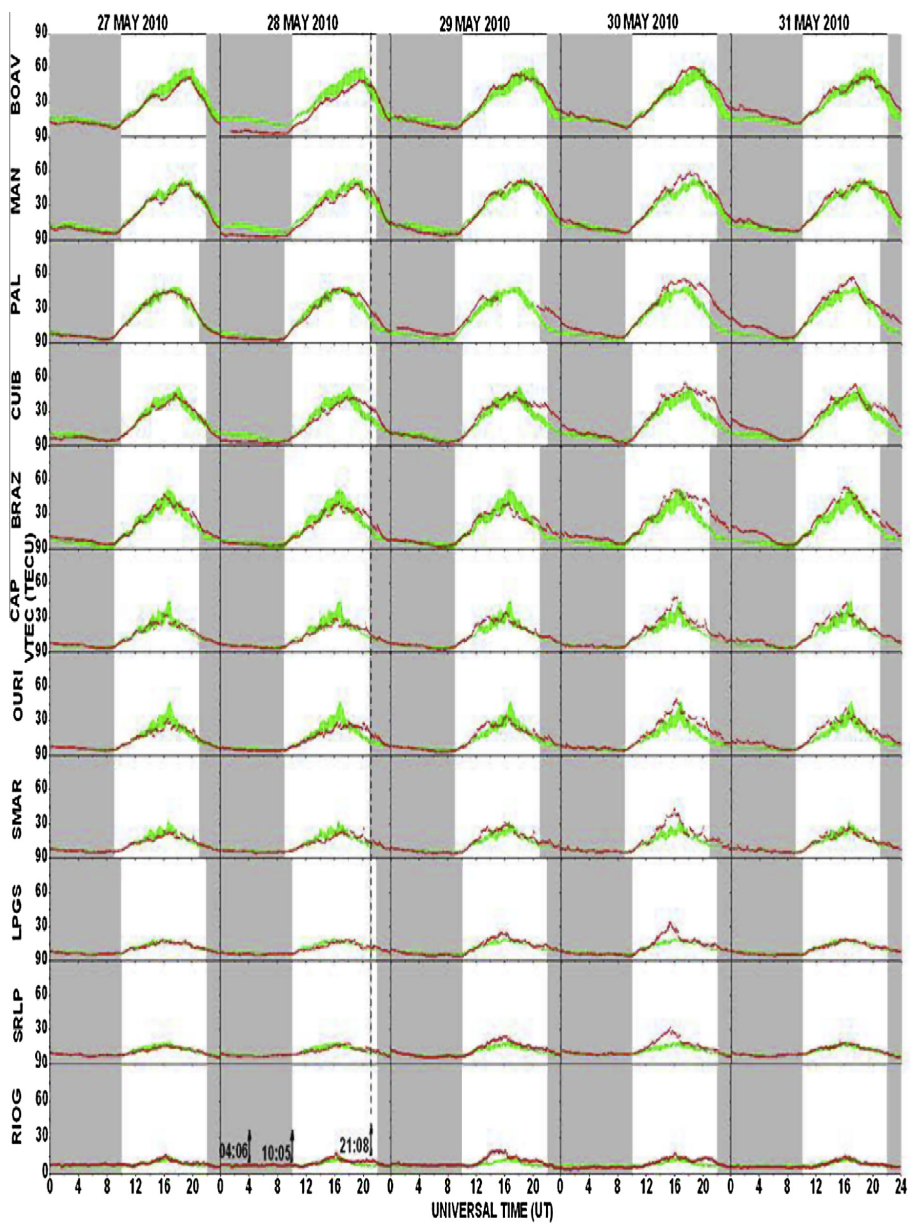

Fig. 9. Variations of the vertical total electron content (VTEC) from GPS observations obtained from different satellites at 11 receiving stations in the South American sector during the period 27–31 May 2010 (red lines). The green bands are ±1 standard deviation of the average quiet day (four quiet days) values. The black vertical arrow and dashed line indicates the gradual storm commencement (GSC). (For interpretation of the references to color in this figure legend, the reader is referred to the web version of this article.)

tigations were obtained from the world data centre (WDC); http://swdcwww.kugi.kyoto-u.ac.jp. The geomagnetic index indicating storm intensity; 3-hourly values (*Kp*) were obtained from http://ftp.gwdg.de./pub/geophys/kp-ap/tab/. The total interplanetary magnetic field (IMF) of the *Bz* component (IMF–*Bz*) in geocentric solar magnetospheric (GSM) coordinates, and solar wind proton bulk velocity (*Vp*) were obtained from the Advanced Composition Explorer (ACE) satellite; http://www.srl.caltech.edu/ace/.

3. Results

Figs. 2 and 8 show the time variability of the solar wind velocity (*Vp*), interplanetary magnetic fields of the *Bz* component (IMF–*Bz*) and geomagnetic indices, auroral electrojet (AE), 3-hourly storm intensity *Kp*, and disturbance storm-time (Dst) for the periods of day 1–4 and 27–31 of May 2010. The black vertical arrow and dashed line indicate the sudden storm commencement (SSC) (Fig. 2) and the gradual storm commencement (GSC) (Fig. 8) of the geomagnetic storm. The average vertical total electron content (VTEC) variability obtained from 15 GPS receiving stations are showed in Figs. 3 and 4 for the period of 1–4 May 2010 and in the Figs. 9 and 10 for the period of 27–31 May 2010. The VTEC values for each station were calculated using satellites with elevation angles greater than 20°. The observed VTEC variations during the disturbed period are shown by a red line. The average VTEC variations for quiet periods (five quiet days: May 21, 22, 23, 24, and 25) are shown with green bands and their widths correspond to ±1 standard deviation (de Jesus et al., 2011). The black vertical arrow and dashed line indicate sudden storm commencement (SSC) (Figs. 3, 4, 6 and 7) and the gradual storm commencement (GSC) (Figs. 9, 10, 12 and 13) of the geomagnetic storm. Figs. 5 and 11 show global TEC maps available every 2 h to investigate the global change in the electron density distribution during the two geomagnetic storms on 01–03 and 27–29 May 2010, respectively. The letters (A) and (B and C) of the figures represent the quiet and disturbed periods, respectively. The phase fluctuations or rate of change of TEC (ROT) are shown in Figs. 6 and 7 for the period of 01–04 May 2010 and in Figs. 12 and 13 for the period of 27–31 May 2010. As pointed out by Aarons et al. (1997), this phase fluctuation indicates the presence of ionospheric irregularities with size in order of kilometers.

3.1. Storm events between 02 and 04 May 2010

Fig. 2 shows that sudden storm commencement (SSC) started at 0909 UT on 02 May 2010. At the same time, the IMF–*Bz* turns southward to a value around −18 nT and there is an increase in solar wind speed from about 375 km/s to about 660 km/s, indicating the arrival of a possible interplanetary shock structure leading to the formation of a geomagnetic storm. After the SSC, the *Kp* index reached 6+ after midday on 02 May 2010 during the main phase of the storm (MPS) and the Dst index was observed decreasing from −21 nT at 1000 UT to −64 nT at 1500 UT

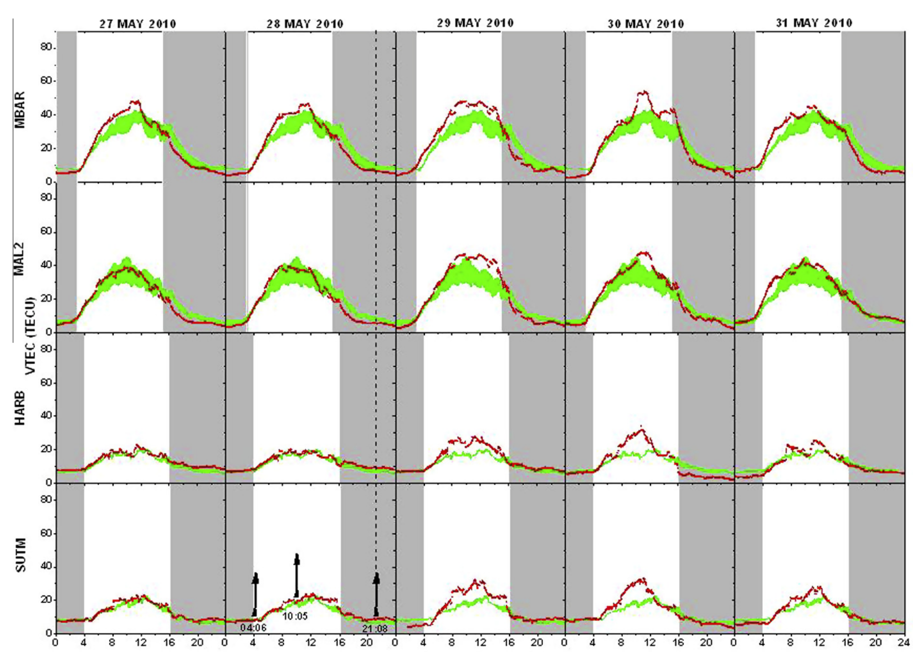

Fig. 10. Variations of the vertical total electron content (VTEC) from GPS observations obtained from different satellites at 4 receiving stations in the African sector during the period 27–31 May 2010 (red lines). The green bands are ±1 standard deviation of the average quiet day (four quiet days) values. The black vertical arrow and dashed line indicates the gradual storm commencement (GSC). (For interpretation of the references to color in this figure legend, the reader is referred to the web version of this article.)

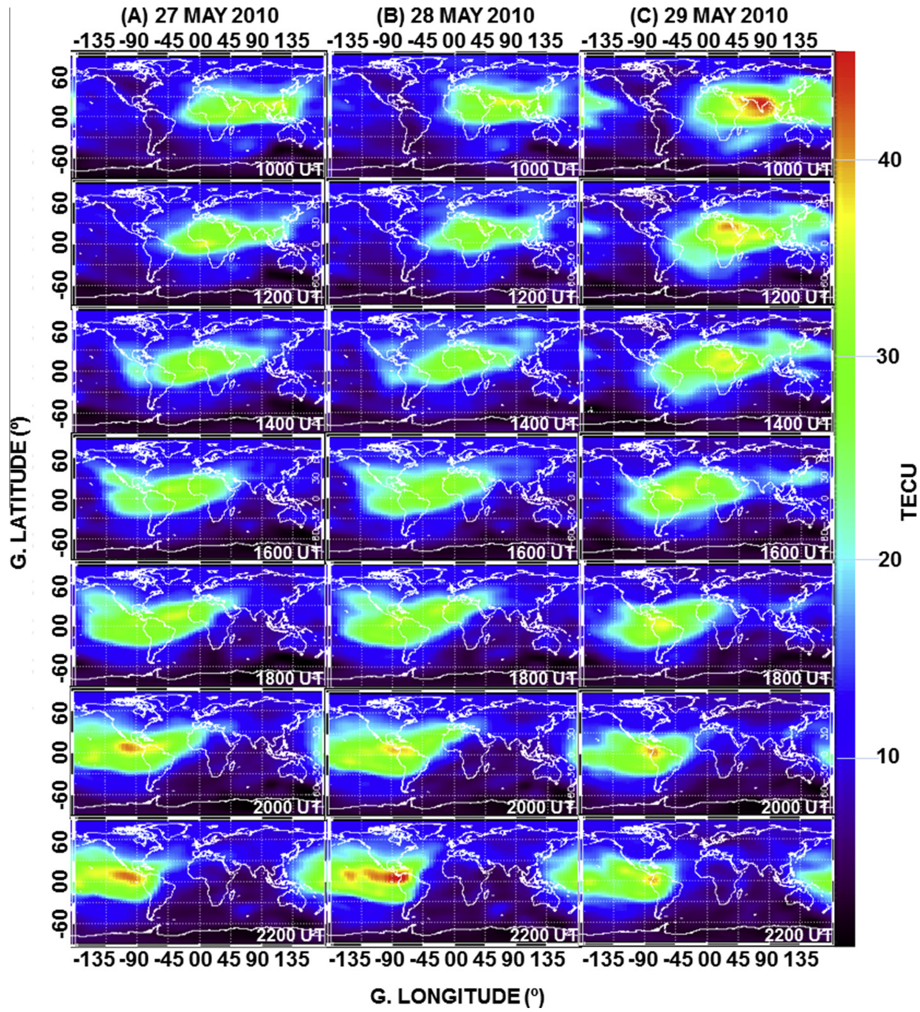

Fig. 11. Twenty-one GPS–TEC maps during the geomagnetic storm on (A) 27 May (geomagnetically quiet) and (B and C) 28–29 May (geomagnetically disturbed).

on 02 May 2010. When rapid changes in the Dst index occur during the MPS, prompt penetration of magnetospheric electric field modifies the ionospheric dynamics at mid-latitude and low-latitudes on the dayside and night side (Basu et al., 2001; Klimenko and Klimenko, 2012; Lu et al., 2012). After 1430 UT on 02 May 2010, a longer recovery phase of the storm (RPS) was observed and terminated at the end on 04 May 2010 (Fig. 2). Longer and stronger fluctuations were also observed from the AE index around 1000 UT on 02 May 2010 (after the SSC) and 0200 UT on 04 May 2010, reaching peaks above 1000 nT (Fig. 2). Similar longer and stronger fluctuations observed by Aksnes et al. (2004) indicated that there are larger injections of energy at auroral latitudes due to Joule heating. Zhou et al. (2011) suggested that this Joule heating appears linearly related with increasing AE index.

Fig. 3 shows the variations of VTEC data obtained at the equatorial, low-, and mid-latitude stations in the South American sector during the period 01–04 May 2010. Immediately after SSC (during MPS), a positive phase is observed in the equatorial, low-, and mid-latitudes regions during daytime on 02 May 2010 from BOAV to CUIB and from RIOG to SMAR. The BRAZ, CAP, and OURI stations showed no significant changes compared to the average values on quiet days. A large positive phase is also observed closer to 2200 UT on 02 May 2010 from PAL to OURI stations. However, such observation at 2200 UT was absent at equatorial stations (BOAV and MAN) and mid-latitude stations (from RIOG to LPGS). During daytime hours, RPS was observed on 03 May 2010 (Fig. 3), such that all GPS stations exhibited positive phases (weaker magnitudes in mid-latitude). Fig. 4 shows the variability of VTEC at the low- and mid-latitude stations in the African sector between 01 and 04 May 2010. During the MPS, a positive daytime phase of the storm was observed at the low- and mid-latitude regions on 02 May 2010 at MBAR, MAL2, HARB, and SUTM. During the long RPS, in the daytime on 03 and 04 May 2010, a positive phase of the storm was also observed at the low- and mid-latitude regions. This is similar to the observed signature during the MPS. Interestingly, a positive phase of the storm was observed a day prior (01 May; a quiet geo-

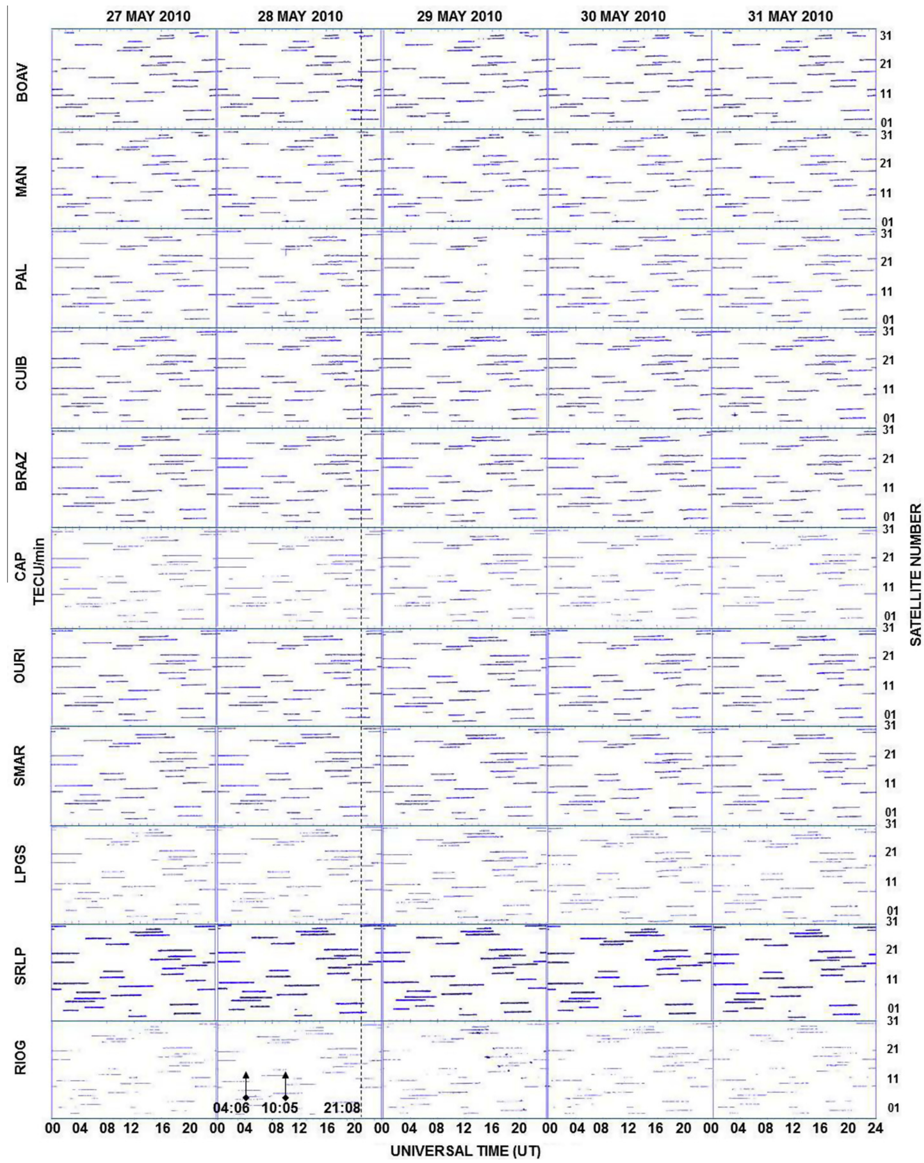

Fig. 12. The phase fluctuations (rate of change of TEC) from GPS observations obtained from different satellites at 11 receiving stations in the South American sector during the period 27–31 May 2010. The black vertical dashed line indicates the gradual storm commencement (GSC).

magnetically day) to the main day when the storm started in the low- and mid-latitudes regions. At the low latitude region on 01 May 2010 this positive phase of the storm occurred with VTEC values slightly lower (around 05 TECU) than those during the main and recovery phases of the storm. However, at the mid-latitude region, VTEC values are almost equal irrespective of the phases of the storms. A positive phase of the storm was also observed on the 04 May 2010 (Fig. 4). This positive phase could be related to the final stage of the RPS when the AE index was undergoing disturbances. However, this positive phase on 04 May 2010 needs further investigation, and detailed study on the day-to-day variability of VTEC in the African sector will be conducted later to highlight possible mechanism that could be responsible for such variability. Hence, this is beyond the scope of this paper.

Fig. 5 shows global TEC maps of the geomagnetic storm on 01–03 May 2010. The comparative study of a quiet period (A) and disturbed periods (B and C) clearly elucidated the effects of these storms on global TEC, focusing mainly on the South American and African sectors. Fig. 6 shows the phase fluctuations of TEC obtained at the equatorial, low-, and mid-latitudes stations in the South American sector during 01–04 May 2010. On the nights of 01–02 (a quiet geomagnetically night), 02–03, and 03–04 May 2010 (main storm and recovery phases, respectively), no phase fluctuations were observed, indicating that the storm did not affect the generation or suppression of ionospheric irregularities in the South American sector. Fig. 7 shows the phase fluctuations of TEC obtained at the low- and mid-latitudes stations in the African sector during the period 01–04 May 2010. Phase fluctuations were observed at MBAR (a low

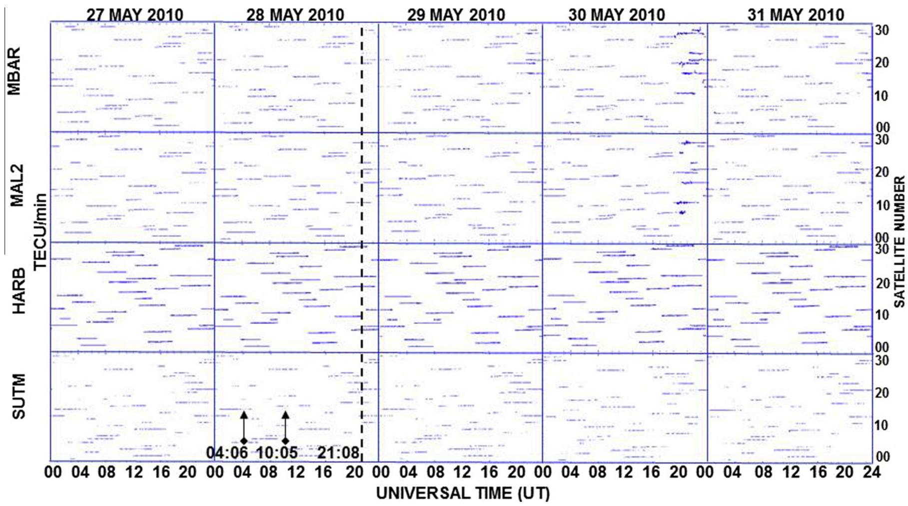

Fig. 13. The phase fluctuations (rate of change of TEC) from GPS observations obtained from different satellites at 04 receiving stations in the African sector during the period 27–31 May 2010. The black vertical dashed line indicates the gradual storm commencement (GSC).

latitude station in Africa) at 1800 UT on the nights of 01–02, 02–03, and 03–04 May 2010. At MAL2 (a low latitude station in Africa), phase fluctuations were observed at 1800 UT on the night of 01–02 May 2010, before a geomagnetic storm. At HARB and SUTM (a mid-latitude station in Africa), no phase fluctuations were observed on the nights of 01–02, 02–03, and 03–04 May 2010. The above results show that the geomagnetic storm observed in the African sector possibly had no influence in the generation of ionospheric irregularities in the equatorial region, which was extended to the low latitude.

3.2. Storm events between 28 and 30 May 2010

Fig. 8 shows two SSC (vertical arrows) followed by two rapid geomagnetic storms. The SSC are related to increases in the solar wind velocity and/or solar wind density (Sahai et al., 2009a). Fig. 8 also shows a third SSC that started at 2108 UT on 28 May 2010. At that same time, the IMF–*Bz* turned southward and reached a value of −15 nT, indicating the arrival of a possible interplanetary shock structure leading to the formation of a geomagnetic storm. However, solar wind velocity remained at 390 km/s during the MPS and RPS. During the MPS, the *Kp* index reached 5+ in the early morning (about 0700 UT) of 29 May 2010 and the Dst index decreased from −3 nT at 2300 UT on 28 May 2010 to about −85 nT at 1400 UT on 29 May 2010. Unlike the previous storm event, when the Dst value decreased rapidly, the Dst value in this case decreased sluggishly. This is not a preferred condition for prompt penetration of magnetospheric electric field into the ionosphere (Basu et al., 2001). After 1400 UT on 29 May 2010, RPS was observed and disappeared around 2300 UT (Fig. 8). Fig. 8 also shows strong fluctuations in the AE index during the MPS and RPS between 2200 UT on 28 May 2010 and 2100 UT on 29 May 2010, when they reached their peaks around 1800 nT. A point worth mentioning is that this geomagnetic storm was followed by two storms of smaller intensity (Dst < −47 nT and Dst < −49 nT) on 30 May 2010. During these two storm periods with smaller intensities, the AE index showed peak values of 1200 nT. As mentioned earlier, AE index is an important indicator and increased values show when greater energy is injected into the auroral latitudes due to Joule heating (Aksnes et al., 2004; Zhou et al., 2011).

The variability of VTEC obtained at the equatorial, low-, and mid-latitudes stations over the South American sector from 27 to 31 May 2010 is shown in Fig. 9. Closer to the end of the MPS and RPS, a positive phase was observed at the equatorial region. This positive phase was significant from BOAV to RIOG between 1200 and 1500 UT. During the RPS on 30 May 2010, a positive phase was observed around 1400 UT and 1800 UT, from the equatorial to mid-latitude regions. A day before and after the commencement of the storm (27 and 31 May 2010, respectively), there was no significant change compared to the average values on quiet days. The variability of VTEC over the African sector between 27 and 31 May 2010 is reported in Fig. 10. Fig. 10 shows that during the MPS and RPS during daytime hours on 29 and 30 May 2010, positive phases were observed between 0800 and 1300 UT at the low- and mid-latitudes regions. However, no significant change was observed on the day before and after the storm on VTEC variability. Comparing both sectors, similar results were observed during moderate storm in the South American and African sectors. Fig. 11 shows global TEC maps of the geomagnetic storm on 27–29 May 2010. Similar to that reported in Fig. 5, the comparative study of A, B, and C exhibit the effect of these storms on global TEC, which support observations showed in Figs. 9 and 10. Figs. 12 and 13 present the phase fluctuations at the equatorial, low-, and mid-latitudes stations over the South American and African sectors between 27 and 31 May 2010. During nighttime on 27–31 May 2010, which are characterized as quiet geomagnetically days, MPS, and RPS, no phase fluctuation was observed. From both the South American and African sectors, it is clearer that the geomagnetic storm during these periods could not initiate generation or suppression of ionospheric irregularities.

4. Discussions and conclusions

Ionospheric storm characteristics are classified into positive and negative phases. Danilov and Morozova (1985), Prolss and Werner (2002) and Korenkov et al. (2012), and references therein suggest that the negative storm phase is associated with O/N_2 density ratio decrease. However, positive storm phase may be influenced by several physical mechanisms, mainly during periods of intense geomagnetic disturbances (Dst < -100 nT). Brief reviews on positive storm phase by Goncharenko et al. (2007), Jones and Rishbeth (1971), Burns et al. (1995b), Huang et al. (2005), and de Abreu et al. (2010a) include increase in the oxygen density, equatorward thermospheric wind, the electric field uplifting the plasma, downward protonospheric plasma fluxes, plasma redistribution from low latitudes by electric field disturbances, and traveling ionospheric disturbances. For the two storm events, from 02 to 04 and 28 to 30 May 2010, the positive storm phases observed in the South American and African sectors indicate that at least one of these aforementioned physical processes are involved during these period. Our results show that the positive storm phases are more prevalent during daytime than the nighttime hours, irrespective of the MPS and RPS (Figs. 3, 4, 9 and 10). How do the moderate storms cause significant changes in the ionospheric electron density?

During the MPS and RPS of these two geomagnetic storms, the global thermospheric wind circulation changes significantly due to increased Joule heating and enhanced energy injection in the auroral zone. The daytime thermospheric wind changes can become equatorward, directly affecting the ionosphere. In Figs. 2 and 8, strong increase in the value of AE index is observed during the MPS and RPS, indicating that higher energy was injected into the high latitude region. It is important to note that due to the fast decrease of the Dst index during the MPS on 02–04 May 2010, there is a possibility of prompt penetration of magnetospheric electric fields into higher latitude of the ionosphere. Therefore, the positive or negative storm effects should be immediate on the ionosphere. However, no effect was observed over the high latitude of the ionosphere. On the other hand, disturbance dynamo electric field is driven by the global thermospheric wind circulation and can persist for many hours due to the neutral-air-inertia (Blanc and Richmond, 1980; Maruyama et al., 2005). Unfortunately, it is not possible to state the exact degree of magnitude of disturbance dynamo electric field in the generation of positive phases observed in the two storm events. Nevertheless, the results presented in this work clearly show that the effects of the equatorward thermospheric wind is the main driver of positive phases of storms in VTEC at equatorial, low-, and mid-latitude regions in the South American and African sectors. As discussed by Balan et al. (2009), the effects of the wind (with and without penetration of electric fields) do not involve changes in thermospheric composition but reduce poleward plasma flow along geomagnetic field lines and raise the ionosphere to high altitudes of reduced chemical loss. This could be the main driver of positive ionospheric storms at low-mid latitudes. Our explanation regarding the mechanism responsible for positive storm phase during daytime hours is supported by several investigators. For example, Lu et al. (2008) used experimental observations (in Millstone Hill and Arecibo) and numerical simulations of ionospheric and thermospheric disturbances that were associated with a moderate geomagnetic storm on 10 September 2005. They reported that the primary cause of a positive storm response during dayside results from the enhanced meridional neutral wind rather than the penetration magnetospheric electric field. de Abreu et al. (2011), using digital ionosonde and GPS observations at the equatorial and low latitude regions over the Brazilian sector during super geomagnetic storm in May 2005, observed positive storm phases during daytime hours. They attributed it to the control by both changes in meridional neutral wind and disturbance dynamo electric fields (Fuller-Rowell et al., 2002; Amabayo et al., 2012). Balan et al. (2010) used multi-instrument observations (in electron density Ne, maximum electron density Nmax, peak density hmax, GPS-TEC, and 630 nm airglow) and theoretical modeling in both Northern and Southern hemispheres of the Japanese–Australian sectors. They suggested that the physical mechanism responsible for these positive ionospheric storms is the equatorward neutral wind. Therefore, our results from this study over the South American and African sectors share similar characteristic with the Japanese–Australia findings. We, therefore, support the suggestion that a thermospheric wind effect is significant on positive ionospheric storms during geomagnetic disturbances.

One of the interesting results from this paper is the positive phase of the geomagnetic storm that was observed from the low- to mid-latitude regions on 01 May 2010 (a day before the geomagnetic storm from 02 to 04 May 2010) over the African sector (Fig. 4). Buresova and Lastovicka (2008) observed several hours up to a day before the onset of geomagnetic storm using ionosonde data in the European area, and they concluded that when the δ foF2 $> 20\%$, this is a typical case of pre-storm, which needs more investigations. Our results show that the δ VTEC $> 70\%$ in the middle of the day before the storm is a case of strong pre-storm enhancement. One of the possible explanations regarding our pre-storm event is related to solar and seasonal variability. The positive storm phase observed before the storm is associated with differences between the solar zenith angle and the F10.7 index. The F10.7 = 78 on 01 May and on 21–25 May (days chosen for the average quiet days) the F10.7 = 70–73, however, more observations are needed to investigate and identify other possible mechanisms that could contribute to production of pre-storm from different sources (Liu et al., 2008a,b).

Our results on ionospheric irregularities are shown in Figs. 6 and 7 (from 02 to 04 May 2010 storm event) and Figs. 12 and 13 (from 28 to 30 May 2010 storm event). These Figs. 6, 7, 12 and 13 show the phase fluctuations of TEC. Studies on phase fluctuations by Aarons et al. (1997) indicated that large-scale ionospheric irregularities are of the order of kilometers. As can be observed from our results, phase fluctuations were significant at low latitude of the African sector. At MBAR, the phase fluctuations were observed throughout every night from 02 to 04 May 2010. However, at MAL2, phase fluctuations were observed a night before the geomagnetic storm from 01 to 02 May 2010. Apart from the observed phase fluctuations in the African sector, no other observation regarding phase fluctuations was seen from all our investigations. This suggests that the ionospheric irregularities were possibly generated in the equatorial region in the African sector due to the pre-reversal enhancement between about 1800 and 2000 LT and observed in the low latitudes at 2100 LT. Thus, these geomagnetic storms could not possibly influence or suppressed the generation of ionospheric irregularities. Considering the variability of ionospheric irregularities, the studies of Abdu (2001), Burke et al. (2004) and Makela and Miller (2008), and references therein, reported that the ionospheric irregularities have seasonal and day-to-day variability. Sahai et al. (2000) also examined seasonal variability of ionospheric irregularities in Brazilian sector using OI 630 nm all-sky imaging system. Their results show maximum values of ionospheric irregularities between October and March and minimal values between May and August. This could a reason why we observed minimal values of phase fluctuations in May 2010. It is important to mention here that geomagnetic storms may also contribute to the generation of ionospheric irregularities, as shown in a study by Sahai et al. (2004) in Brazilian sector using OI 630 nm all-sky imaging system. They analyzed the years between 1987 and 2000 and observed that, during low spread-F season, large-scale ionospheric depletions during geomagnetic storms might be associated with prompt penetration of the magnetospheric convective electric fields. Hence, in our future work, we will study phase fluctuations and spread-F over South America and Africa simultaneously for a whole year to ascertain their monthly maximum and minimum values. This will also include the role of the geomagnetic storms in the generation and suppression of ionospheric irregularities.

In conclusion, the responses of the ionospheric F region at equatorial, low-, and mid-latitude regions over the South American and African sectors during two moderate geomagnetic storms in May 2010 were investigated. The responses during the ascending phase of solar cycle 24 were related to the phenomena of ionospheric storms as well as generations and suppressions of equatorial ionospheric irregularities. Therefore, the study showed that the features of these two moderate storms in May 2010 at the equatorial, low-, and mid-latitude regions over South America and Africa are significant. They show positive ionospheric storms in daytime during the main and recovery phases of the geomagnetic storms. Our results also found a pre-storm event on 01 May 2010 over the African sector. In addition, this study showed that there was no generation or suppression of ionospheric irregularities during storm events. Hence, further studies are needed to fully understand the suppression and generation of ionospheric irregularities during moderate geomagnetic storms. This will include months when an ionospheric irregularity is expected to be higher.

Acknowledgements

The authors thank the authorities of the “Rede Brasileira de Monitoramento Contínuo de GPS (RBMC)”, Brazil; “Serviço de Referência Geocêntrico para as Américas (SIRGAS)”, Argentina; and International Global Navigation Satellite System (GNSS) Service (IGS) for easy access to their data. We are also grateful to the Brazilian funding agency “Fundação de Amparo à Pesquisa do Estado de São Paulo – FAPESP (process number 2011/20270-7)” for kindly providing partial financial support to carry out this work.

References

Aarons, J., Mendillo, M., Yantosca, R., 1996. GPS phase fluctuations in the equatorial region during the MISETA 1994 campaign. J. Geophys. Res. 101 (A8), 26,851–26,862.

Aarons, J., Mendillo, M., Yantosca, R., 1997. GPS phase fluctuations in the equatorial region during sunspot minimum. Radio Sci. 32, 1535–1550. http://dx.doi.org/10.1029/97RS00664.

Abdu, M.A., Walker, G.O., Reddy, B.M., de Paula, E.R., Sobral, J.H.A., Fejer, B.G., 1993. Global scale equatorial ionization anomaly (EIA) response to magnetospheric disturbances based on the May–June 1987 SUNDIAL-coordinated observations. Ann. Geophys. 11, 585–594.

Abdu, M.A., 1997. Major phenomena of the equatorial ionosphere–thermosphere system under disturbed conditions. J. Atmos. Sol. Terr. Phys. 5 (13), 1505–1519.

Abdu, M.A., 2001. Outstanding problems in the equatorial ionosphere–thermosphere electrodynamics relevant to spread F. J. Atmos. Sol. Terr. Phys. 63, 869–884.

Aksnes, A., Stadsnes, J., Lu, G., Østgaard, N., Vondrak, R.R., Detrick, D.L., Rosenberg, T.J., Germany, G.A., Schulz, M., 2004. Effects of energetic electrons on the electrodynamics in the ionosphere. Ann. Geophys. 22, 475–496.

Amabayo, E.B., McKinnell, L.-A., Cilliers, P.J.J., 2012. Atmos. Sol. Terr. Phys. 84–85, 62–74.

Balan, N., Alleyne, H., Otsuka, Y., Vijaya Lekshmi, D., Fejer, B.G., McCrea, I., 2009. Relative effect of electric field and neutral wind on positive ionospheric storms. Earth Planets Space 61, 439–445.

Balan, N., Shiokawa, K., Otsuka, Y., Kikuchi, T., Vijaya Lekshmi, D., Kawamura, S., Yamamoto, M., Bailey, G.J., 2010. A physical mechanism of positive ionospheric storms at low latitudes and midlatitudes. J. Geophys. Res. 115 (A2).

Blanc, M., Richmond, A.D., 1980. The ionospheric disturbance dynamo. J. Geophys. Res. 85, 1669–1686.

Basu, S., Basu, Su., Valladares, C.E., Yeh, H.-C., Su, S.-Y., Mackenzie, E., Sultan, P.J., Aarons, J., Rich, F.J., Doherty, P., Groves, K.M., Bullet, T.W., 2001. Ionospheric effects of major magnetic storms during the international space weather period of September and October 1999: GPS observations, VHF/UHF scintillations, and in situ density structures at middle and equatorial latitudes. J. Geophys. Res. 106 (A12), 30,389–30,413.

Basu, S., Basu, Su., Rich, F.J., Groves, K.M., MacKenzie, E., Coker, C., Sahai, Y., Fagundes, P.R., Becker-Guedes, F., 2007. F response of the equatorial ionosphere at dusk to penetration electric fieldsduring intense magnetic storms. J. Geophys. Res. 112 (A8). http://dx.doi.org/10.1029/2006JA012192. Art. No. A08308 2007.

Bauske, R., Prolss, G.W., 1998. Numerical simulation of long-duration positive ionospheric storm effects. Adv. Space Res. 22 (1), 117–121.

Brunini, C., Meza, A., Gende, M., Azpilicueta, F., 2008. South American regional ionospheric maps computed by GESA: a pilot service in the framework of SIRGAS. Adv. Space Res. 42, 737–744.

Buresova, D., Lastovicka, J., 2008. Pre-storm enhancements of foF2 above Europe. Adv. Space Res. 39, 1298–1303.

Burke, W.J., Huang, C.Y., Gentile, L.C., Bauer, L., 2004. Seasonal–longitudinal variability of equatorial plasma bubbles. Ann. Geophys. 22, 3089–3098.

Burns, A.G., Killeen, T.L., Deng, W., Carignan, G.R., Roble, R.G., 1995a. Geomagnetic storm effects in the low- to middle latitude upper thermosphere. J. Geophys. Res. 100 (A8), 14673–14691.

Burns, A.G., Killeen, T.L., Carignan, G.R., Roble, R.G., 1995b. Large enhancements in the O/N_2 ratio in the evening sector of the winter hemisphere during geomagnetic storms. J. Geophys. Res. 100, 14,661–14,671.

Danilov, A.D., Morozova, L.D., 1985. Ionospheric storms in the F2 region: morphology and physics (review). Geomag. Aeron. 25, 593–605.

de Abreu, A.J., Fagundes, P.R., Sahai, Y., de Jesus, R., Bittencourt, J.A., Brunini, C., Gende, M., Pillat, V.G., Lima, W.L.C., Abalde, J.R., Pimenta, A.A., 2010a. Hemispheric asymmetries in the ionospheric response observed in the American sector during an intense geomagnetic storm. J. Geophys. Res. 115, A12312. http://dx.doi.org/10.1029/2010JA015661.

de Abreu, A.J., Sahai, Y., Fagundes, P.R., Becker-Guedes, F., de Jesus, R., Guarnieri, F.L., Pillat, V.G., 2010b. Response of the ionospheric F-region in the Brazilian sector during the super geomagnetic storm in April 2000 observed by GPS. Adv. Space Res. 45, 1322–1329. http://dx.doi.org/10.1016/j.asr.2010.02.003.

de Abreu, A.J., Sahai, Y., Fagundes, P.R., de Jesus, R., Bittencourt, J.A., Pillat, V.G., 2011. An investigation of ionospheric F region response in the Brazilian sector to the super geomagnetic storm of May 2005. Adv. Space Res. 48, 1211–1220.

de Jesus, R., Sahai, Y., Guarnieri, F.L., Fagundes, P.R., de Abreu, A.J., Becker-Guedes, F., Brunini, C., Gende, M., Cintra, T.M.F., de Souza, V.A., Pillat, V.G., Lima, W.L.C., 2010. Effects observed in the ionospheric F-region in the South American sector during the intense geomagnetic storm of 14 December 2006. Adv. Space Res. 46, 909–920. http://dx.doi.org/10.1016/j.asr.2010.04.031.

de Jesus, R., Sahai, Y., Guarnieri, F.L., Fagundes, P.R., de Abreu, A.J., Pillat, V.G., Lima, W.L.C., 2011. F-region ionospheric parameters observed in the equatorial and low latitude regions during médium solar activity in the Brazilian sector and comparison with the IRI-2007 model results. Adv. Space Res. 47, 718–728.

de Jesus, R., Sahai, Y., Guarnieri, F.L., Fagundes, P.R., de Abreu, A.J., Bittencourt, J.A., Nagatsuma, T., Huang, C.-S., Lan, H.T., Pillat, V.G., 2012. Ionospheric response of equatorial and low latitude F-region during the intense geomagnetic storm on 24–25 August 2005. Adv. Space Res. 49, 518–529.

de Jesus, R., Sahai, Y., Fagundes, P.R., de Abreu, A.J., Brunini, C., Gende, M., Bittencourt, J.A., Abalde, J.R., Pillat, V.G., 2013. Response of equatorial, low- and mid-latitude F-region in the American sector during the intense geomagnetic storm on 24–25 October 2011. Adv. Space Res. 52, 147–157. http://dx.doi.org/10.1016/j.asr.2013.03.017.

Dow, J.M., Neilan, R.E., Gendt, G., 2005. The international GPS service (IGS): celebrating the 10th anniversary and looking to the next decade. Adv. Space Res. 36 (3), 320–326.

Fagundes, P.R., Aruliah, A.L., Rees, D., Bittencourt, J.A., 1995. Gravity-wave generation and propagation during geomagnetic storms over Kiruna (67.8°N, 20.4°E). Ann. Geophys. 13 (4), 358–366.

Fejer, B.G., Jensen, J.W., Kikuchi, T., Abdu, M.A., Chau, L., 2007. Equatorial ionospheric electric fields during the November 2004 magnetic storm. J. Geophys. Res. 112, A10304. http://dx.doi.org/10.1029/2007JA012376.

Fuller-Rowell, T.J., Codrescu, M.V., Moffet, R.J., Quegan, S., 1994. Response of the thermosphere and ionosphere to geomagnetic storms. J. Geophys. Res. 99 (A3), 3893–3914.

Fuller-Rowell, T.J., Millward, G.H., Richmond, A.D., Codrescu, M.V., 2002. Storm-time changes in the upper atmosphere at low latitudes. Atmos. Sol. Terr. Phys. 64, 1383–1391.

Goncharenko, L.P., Foster, J.C., Coster, A.J., Huang, C., Aponte, N., Paxton, L.J., 2005. Observations of a positive storm phase on September 10, 2005. J. Atmos. Sol. Terr. Phys. 69, 1253–1272.

Goncharenko, L.P., Foster, J.C., Coster, A.J., Huang, C., Aponte, N., Paxton, L.J., 2007. Observations of a positive storm phase on September 10, 2005. J. Atmos. Sol. Terr. Phys. 69, 1253–1272.

Gonzalez, W.D., Tsurutani, B.T., 1987. Criteria of interplanetary parameters causing intense magnetic storms (Dst < -100 nT). Planet. Space Sci. 35 (9), 1101–1109.

Huang, C.-S., Foster, J.C., Goncharenko, L.P., Erickson, P.J., Rideout, W., Coster, A.J., 2005. Strong positive phase of ionospheric storms observed by the Millstone Hill incoherent scatter radar and global GPS network. J. Geophys. Res. 110 (A6), A06303.

Huang, C.M., 2013. Disturbance dynamo electric fields in response to geomagnetic storms occurring at different universal times. J. Geophys. Res. 118, 496–501. http://dx.doi.org/10.1029/2012JA018118.

Jones, K.L., Rishbeth, H., 1971. The origin of storm increases of mid-latitude F-layer electron concentration. J. Atmos. Terr. Phys. 33, 391–401.

Karpachev, A.T., Beloff, N., Carozzi, T.D., Denisenko, P.F., Karhunen, T.J.T., Lester, M., 2010. Detection of large scale TIDs associated with the dayside cusp using SuperDARN data. J. Atmos. Sol. Terr. Phys. 72 (9/10), 653–661.

Killeen, T.J., Hays, P.B., Carignan, G.R., Heelis, R.A., Hanson, W.B., Spencer, N.W., Brace, L.H., 1984. Ion-neutral coupling in the high-latitude F-region: evaluation of ion heating terms from dynamics explorer 2. J. Geophys. Res. 89, 7495–7508.

Klimenko, M.V., Klimenko, V.V., Ratovsky, K.G., Goncharenko, L.P., Sahai, Y., Fagundes, P.R., de Jesus, R., de Abreu, A.J., Vesnin, A.M., 2011. Numerical modeling of ionospheric effects in the middle- and low-latitude F region during geomagnetic storm sequence of 9–14 September 2005. Radio Sci. http://dx.doi.org/10.1029/2010RS004590.

Klimenko, M.V., Klimenko, V.V., 2012. Disturbance dynamo, prompt penetration electric field and overshielding in the Earth's ionosphere during geomagnetic storm. J. Atmos. Sol. Terr. Phys. 90–91, 146–155. http://dx.doi.org/10.1016/j.jastp.2012.02.018, ISSN 1364–6826.

Korenkov, Y.N., Klimenko, V.V., Klimenko, M.V., Bessarab, F.S., Korenkova, N.A., Ratovsky, K.G., Chernigovskaya, M.A., Shcherbakov, A.A., Sahai, Y., Fagundes, P.R., de Jesus, R., de Abreu, A.J., Condor, P., 2012. The global thermospheric and ionospheric response to the 2008 minor sudden stratospheric warming event. J. Geophys. Res. 117, A10309.

Kumar, S., Chandra, H., Sharma, S., 2005. Geomagnetic storms and their ionospheric effects observed at the equatorial anomaly crest in the Indian Region. J. Atmos. Sol. Terr. Phys. 67, 581–594.

Liu, L., Wan, W., Zhang, M.-L., Zhao, B., Ning, B., 2008a. Prestorm enhancements in NmF2 and total electron content at low latitudes. J. Geophys. Res. 113, A02311.

Liu, L., Wan, W., Zhang, M.-L., Zhao, B., 2008b. Case study on total electron content enhancements at low latitudes during low geomagnetic activities before the storms. Ann. Geophys. 26, 893–903.

Lu, G., Goncharenko, L., Richmond, A.D., Roble, R.G., Aponte, N., 2008. A dayside ionospheric positive storm phase driven by neutral winds. J. Geophys. Res. 113, A8.

Lu, G., Goncharenko, L., Nicolls, M.J., Maute, A., Coster, A., Paxton, L.J., 2012. Ionospheric and thermospheric variations associated with prompt penetration electric field. J. Geophys. Res. 117 (A8), 1978–2012.

Makela, J.J., Miller, E.S., 2008. Optical observations of the growth and day-to-day variability of equatorial plasma bubbles. J. Geophys. Res. 113, A03307.

Maruyama, N., Richmond, A.D., Fuller-Rowell, T.J., Codrescu, M.V., Sazykin, S., Toffoletto, F.R., Spiro, R.W., Millward, G.H., 2005. Interaction between direct penetration and disturbance dynamo electric fields in the storm-time equatorial ionosphere. J. Geophys. Res. 32, L17105. http://dx.doi.org/10.1029/2005GL023763.

Mendillo, M., 2006. Storms in the ionosphere: patterns and processes for total electron content. American Geophysical Union, vol. 44, No. 2005RG000193, p. 47.

Ngwira, C.M., McKinnell, L.-A., Cilliers, P.J., Yizengaw, E., 2012. An investigation of ionospheric disturbances over South Africa during the magnetic storm on 15 May 2005. Adv. Space Res. 49.

Namgaladze, A.A., Forster, M., Yurik, R.Y., 2000. Analysis of the positive ionospheric response to a moderate geomagnetic storm using a global numerical model. Ann. Geophys. 18, 461–477.

Prolss, G.W., 1993. Common origin of positive ionospheric storms at middle latitudes and the geomagnetic activity effect at low latitudes. J. Geophys. Res. 98 (A4), 5981–5991.

Prolss, G.W., Werner, S., 2002. Vibrationally excited nitrogen and oxygen and the origin of negative ionospheric storms. J. Geophys. Res. Space Phys. 107 (A2). http://dx.doi.org/10.1029/2001JA900126. Art. No. 1016.

Richmond, A.D., Lu, G., 2000. Upper-atmospheric effects of magnetic storms: a brief tutorial. J. Atmos. Sol. Terr. Phys. 62, 1115–1127.

Richmond, A.D., Peymirat, C., Roble, R.G., 2003. Long-lasting disturbances in the equatorial ionospheric electric field simulated with a coupled magnetosphere–ionosphere–thermosphere model. J. Geophys. Res. 108 (A3), SIA5/1–SIA5/12.

Sahai, Y., Fagundes, P.R., Bittencourt, J.A., 2000. Transequatorial F-region ionospheric plasma bubbles: solar cycle effects. J. Atmos. Sol. Terr. Phys. 62, 1377–1383.

Sahai, Y., Fagundes, P.R., Abalde, J.R., Pimenta, A.A., Bittencourt, J.A., Otsuka, Y., Rios, V.H., 2004. Generation of large-scale equatorial F-region plasma depletions during low range spread-F season. Ann. Geophys. 22, 15–23.

Sahai, Y., Becker-Guedes, F., Fagundes, P.R., Lima, W.L.C., Otsuka, Y., Huang, C.-S., Espinoza, E.S., Pi, X., de Abreu, A.J., Bolzan, M.J.A., Pillat, V.G., Abalde, J.R., Pimenta, A.A., Bittencourt, J.A., 2007a. Response of nighttime equatorial and low latitude F-region to the geomagnetic storm of August 18, 2003, in the Brazilian sector. Adv. Space Res. 39, 1325–1334.

Sahai, Y., Becker-Guedes, F., Fagundes, P.R., Lima, W.L.C., de Abreu, A.J., Pillat, V.G., 2007b. Unusual ionospheric effects observed in the Brazilian sector during the October 2003 solar flare. Ann. Geophys. 25, 2497–2502.

Sahai, Y., Becker-Guedes, F., Fagundes, P.R., de Jesus, R., de Abreu, A.J., Paxton, L.J., Goncharenko, L.P., Brunini, C., Gende, M., Ferreira, A.S., Lima, N.S., Guarnieri, F.L., Pillat, V.G., Bittencourt, J.A., Candido, C.M.N., 2009a. Effects observed in the Latin American sector ionospheric F region during the intense geomagnetic disturbances in the early part of November 2004. J. Geophys. Res. 114, A00A19.

Sahai, Y., Becker-Guedes, F., Fagundes, P.R., de Abreu, A.J., de Jesus, R., Pillat, V.G., Abalde, J.R., Martinis, C.R., Brunini, C., Gende, M., Huang, C.S., Pi, X., Lima, W.L.C., Bittencourt, J.A., Otsuka, T., 2009b. Observations of the F-region ionospheric irregularities in the South American sector during the October 2003 'Halloween Storms'. Ann. Geophys. 27 (12), 4463–4477.

Sahai, Y., Becker-Guedes, F., Fagundes, P.R., de Jesus, R., de Abreu, A.J., Otsuka, Y., Shiokawa, K., Igarashi, K., Yumoto, K., Huang, C.S., Lan, H.T., Saito, A., Guarnieri, F.L., Pillat, V.G., Bittencourt, J.A., 2009c. Effects observed in the ionospheric F region in the east Asian sector during the intense geomagnetic disturbances in the early part of November 2004. J. Geophys. Res. Space Phys. 114. http://dx.doi.org/10.1029/2008JA013053. Art. No. A00A18.

Sahai, Y., Fagundes, P.R., de Jesus, R., de Abreu, A.J., Crowley, G., Kikuchi, T., Huang, C.-S., Pillat, V.G., Guarnieri, F.L., Abalde, J.R., Bittencourt, J., 2011. Studies of ionospheric F-region response in the Latin American sector during the geomagnetic storm of 21–22 January 2005. Ann. Geophys. 29, 1–11. http://dx.doi.org/10.5194/angeo-29-1-2011.

Sastri, J.H., Niranjan, K., Subbarao, K.S.V., 2002. Response of the equatorial ionosphere in the Indian (midnight) sector to the severe magnetic storm of July 15, 2000. Geophys. Res. Lett. 29 (13), 1651. http://dx.doi.org/10.1029/2002GL015133.

Schunk, R.W., Nagy, A.F., 2000. Ionospheres: Physics, Plasma Physics and Chemistry. Cambridge University Press, USA.

Simi, K.G., Manju, G., Haridas, M.K.M., Nayar, S.R.P., Pant, T.K., Alex, S., 2013. Ionospheric response to a geomagnetic storm during November 8–10, 2004. Earth Planets Space 65, 343–350. http://dx.doi.org/10.5047/eps.2012.09.005.

Tsurutani, B.T., Gonzalez, W.D., 1997. The interplanetary cause of magnetic storms: a review. In: Tsurutani, B.T., Gonzalez, W.D., Kamide, Y., Arballo, J.K. (Eds.), Magnetic Storms, Washington, DC, vol. 98.

Tsurutani, B.T., Mannucci, A., Iijima, B., Abdu, M.A., Sobral, J.H.A., Gonzalez, W., Guarnieri, F.L., Tsuda, T., Saito, A., Yumoto, K., Fejer, B., Fuller-Rowell, T.J., Kozyra, J., Foster, J.C., Coster, A., Vasyliunas, V.M., 2004. Global dayside ionospheric uplift and enhancement associated with interplanetary electric fields. J. Geophys. Res. 109, A08302.

Uma, G., Brahmanandam, P.S., Kakinami, Yoshihiro, Dmitriev, A., Latha Devi, N.S.M.P., Uday Kiran, K., Prasad, D.S.V.V.D., Rama Rao, P.V.S., Niranjan, K., Seshu Babu, Ch., Chu, Y.H., 2012. Ionospheric responses to two large geomagnetic storms over Japanese and Indian longitude sectors. J. Atmos. Sol. Terr. Phys. 74, 94–110. http://dx.doi.org/10.1016/j.jastp.2011.10.001, ISSN 1364-6826.

Wanninger, L., 1993. Effects of the Equatorial Ionosphere on GPS, GPS World, p. 48–54.

Werner, S., Bauske, R., Prolss, G.W., 1999. On the origin of positive ionospheric storms. Adv. Space Res. 24 (11), 1485–1489.

Whalen, J.A., 2002. Dependence of equatorial bubbles and bottom-side spread F on season, magnetic activity, and E × B drift velocity during solar maximum. J. Geophys. Res. 107, A2.

Willis, D.M., 1964. The sudden commencement and first phase of a geomagnetic storm. J. Atmos. Terr. Phys. 26, 581–602.

Zaka, K.Z., Kobea, A.T., Doumbia, V., Richmond, A.D., Maute, A., Mene, N.M., Obrou, O.K., Assamoi, P., Boka, K., Adohi, J.-P., Amory-Mazaudier, C., 2010. Simulation of electric field and current during the 11 June 1993 disturbance dynamo event: comparison with the observations. J. Geophys. Res. 115, A11307. http://dx.doi.org/10.1029/2010JA015417.

Zhou, X.-Y., Sun, W., Ridley, A.J., Mende, S.B., 2011. Joule heating associated with auroral electrojets during magnetospheric substorms. J. Geophys. Res. 116 (A5), 1978–2012.